Biochemical and Biophysical Research Communications 440 (2013) 62–67

Contents lists available at ScienceDirect

Biochemical and Biophysical Research Communications

journal homepage: www.elsevier.com/locate/ybbrc

Induction of senescence by adenosine suppressing the growth of lung cancer cells

Dongqin Yang [a,1], Junyao Song [b,1], Lijun Wu [a], Yunfang Ma [a], Chunhua Song [c], Sinisa Dovat [c], Tomoyuki Nishizaki [d], Jie Liu [a,*]

[a] Department of Digestive Diseases, Huashan Hospital, Fudan University, Shanghai 200040, China
[b] Center for Biomedical Engineering, Massachusetts Institute of Technology, Cambridge, MA 02139, USA
[c] Department of Pediatrics, Pennsylvania State University College of Medicine, Hershey, PA 17033, USA
[d] Division of Bioinformation, Department of Physiology, Hyogo College of Medicine, 1-1 Mukogawa-cho, Nishinomiya 663-8501, Japan

ARTICLE INFO

Article history:
Received 23 August 2013
Available online 17 September 2013

Keywords:
Adenosine
Cellular senescence
A549 cell
DNA damage

ABSTRACT

Extracellular adenosine is well reported to suppress tumor growth by induction of apoptosis. However, in this study we found that adenosine treatment results in cellular senescence in A549 lung cancer cells both *in vitro* and *in vivo*; adenosine induces cell cycle arrest and senescence in a p53/p21 dependent manner; adenosine elevates the level of phosphor-γH2AX, pCHK2 and pBRCA1, the markers for prolonged DNA damage response which are likely responsible for initiating the cellular senescence. Our study first demonstrates that adenosine suppresses growth of cancer cells by inducing senescence and provides additional evidence that adenosine could act as an effective anticancer agent for targeted cancer therapy.

1. Introduction

Adenosine, a metabolite of ATP that is abundantly present inside and outside cells, is reported to suppress cell growth through apoptosis in a variety of cancer cells via diverse extrinsic and intrinsic signaling pathways [1]. Adenosine induces apoptosis via extrinsic pathways in mouse astrocytoma cells, human colonic cancer cells, glioma cells, myeloid leukemia cells, mammary carcinoma cells, lung cancer cells and thyroid cancer cells [1]. Through intrinsic pathways, intracellularly transported adenosine induces apoptosis in GT3-TKB human lung cancer cells [2], HuH-7 human hepatoma cells [1] and HepG2 human hepatoma cells [3]. In both extrinsic and intrinsic pathways, adenosine activates caspases in a mitochondria-dependent and/or independent manner [3]. The biochemical mechanisms for adenosine action in apoptosis are well clarified; however it is unknown whether adenosine can suppress cell growth by a mechanism other than induction of apoptosis in tumor cells.

Cellular senescence is defined as an irreversible growth arrest with specific cellular morphology and gene expression patterns [4,5]. Various stimuli such as telomere dysfunction [6], oncogene activation [7], DNA damage [8], and several chemotherapeutic drugs can contribute to cellular senescence [9]. Cellular senescence is one of the major mechanisms that prevent aged cells or cells bearing mutations from expanding, and it is also a major barrier that cells must overcome in order to progress to full-blown malignancy [10].

Recent findings indicate that the major mechanism by which many cancer drugs exert their anti-tumor effect is by inducing cellular senescence following DNA damage [11]. DNA damage results in the phosphorylation of ATM/ATR, and activation of H2AX, and BRCA1, followed by activation of Chk1 and Chk2, resulting in cell cycle arrest [8,12]. The p16/pRB and p53/p21 axes are the two major senescence-triggering pathways in response to stresses [13,14]. Here, we report that adenosine triggers senescence in lung cancer cells, an irreversible and p53/p21 dependent process that is likely a consequence of increased phosphor-γH2AX, pCHK2 and pBRCA1, the markers for prolonged DNA damage response. Our study demonstrates that adenosine suppresses the growth of cancer cells by inducing senescence and that adenosine could act as an effective anticancer agent for targeted cancer therapy.

2. Materials and methods

2.1. Cell line and cell culture

Human lung adenocarcinoma cell line A549 was obtained from the American Type Culture Collection (ATCC, Rockville, Maryland, U.S.A.), and was cultured in RPMI-1640 (Hyclone, Beijing, China) supplemented with 10% heat-inactivated fetal bovine serum at 37 °C in a humidified air atmosphere with 5% CO_2.

* Corresponding author.
E-mail address: jieliu@fudan.edu.cn (J. Liu).
[1] D Yang and J Song are co-first authors of this article.

0006-291X/$ - see front matter © 2013 Elsevier Inc. All rights reserved.
http://dx.doi.org/10.1016/j.bbrc.2013.09.030

P53-RE-Fluc/A549 cell line was kindly provided by Caliper Company (Caliper Life Sciences, Inc.,CA). Three tandem repeats of p53 response element which can bind with chemotherapy drugs were linked with a minimal TK promoter and the luciferase structural gene. The lentivirus was stably transfected into human lung carcinoma cell line A549 cells to obtain the p53-RE-Fluc/A549 cell line. As a result, the expression level of firefly luciferase (fluc) directly reflects p53 activity, which can be measured by bioluminescent Imaging (BLI). The p53-RE-Fluc/A549 cells were cultured the same as A549 cells.

2.2. Cell viability assay and detection growth curves and cell cycle assay

A549 cells were plated on 96-well plates (Corning) at a density of 3×10^3 cells per well and treated with adenosine at different concentrations (0.1–10 mM). After 1 day, MTT (10 μl, 5 mg/ml; Sigma) was added into each well and the plates were placed in a 37 °C incubator for 3 h. Following that, the medium was discarded and 100 μl DMSO (Sigma) was added. The absorbance at wavelength 570 nm was measured using a Microplate Reader (Thermo).

Growth curves were made using the Incucyte instrument (Ann Arbor, MI). Cells were plated in a 96-well plate and treated with 10 mM adenosine or untreated as an control. Then the plate was inserted into the Incucyte instrument. Each well was detected and imaged every other hour, and photographs of 24 h were selected as morphologic images.

Cells were harvested and fixed in 70% ethanol at −20 °C overnight and then stained with propidium iodide (36 μg/mL, Sigma) containing 400 μg/mL, RNAase (Roche) with shaking for 1 h and analyzed by flow cytometry (CyAn™ ADP, Beckman Coulter) for cell cycle analysis as previously reported [1,15].

2.3. Senescence-associated β-galactosidase

To determine cellular senescence, A549 cells were plated at 10^5 cells per well in a 6-well plate and either untreated or treated with 10 mM adenosine. After 8 h or 24 h, SA-β-gal activity was measured with a senescence-associated β-Galactosidase Staining Kit (Beyotime, China) and quantified (around 200 cells per well). For detection of SA-β-gal activity in p21 knockdown cells, the cells were treated with p21 siRNA (100 nM) or control siRNA (100 nM) for 72 h and then treated with 10 mM adenosine for 24 h. For the assay in MRS1523 treated cells, the cells were treated with MRS1523 (50 μM) and adenosine (10 mM) for 24 h. For *in vivo* cellular senescence detection, frozen sections 10 μm-thick were used and stained. The images were taken from an OLYMPUS BX51 microscope (OLYMPUS, Tokyo, Japan).

2.4. Animal experiments

Animal experiments were operated in accordance with the National Institutes of Health Guide for the Care and Use of Laboratory Animals. Female BALB/c nude mice (4 to 5-weeks old) were obtained from Shanghai Experimental Animal Center (Shanghai, China). 5×10^6 A549 cells were subcutaneously injected into each mouse to establish xenograft tumors. Animals were divided into two groups at random (ten mice per group) and treated with PBS or adenosine every other day for 12 times. The tumor volume was measured once a week and calculated as follows: tumor volume (mm^3) = (length × width^2)/2. When the experiment was finished, all mice were sacrificed and their tumor tissues were dissected and weighed. The tumor tissues were saved for further immunohistological staining and biochemical experiments.

2.5. Bioluminescence imaging

Cells (1×10^6) were suspended in PBS (100 μL) and injected (s.c.) into the flanks of nude mice. After the tumors were formed at 24 h, mice were transiently injected with adenosine (i.p., 50 mg/kg) or PBS and measured by a caliper at 0, 8 and 24 h. Nude mice were injected with D-luciferin solution (i.p., 125 mg/kg), anesthetized by isoflurane, and imaged at different time points as described above. Fluc radiance was detected by the Xenogen IVIS Kinetics imaging system (Caliper Life Sciences, Inc.).The results were analyzed by the IVIS Living Imaging software package (Caliper Life Sciences, Inc.), and the optical signal was expressed as total radiance in units of p/s/cm^2/sr within the region of interest.

2.6. Immunofluorescence

A549 cells were seeded on glass coverslips in a 24-well plate and were either untreated or treated with 10 mM adenosine for 1 day. The cells were fixed in 4% paraformaldehyde, permeabilized in 0.1% Triton-X before staining, blocked with 10% donkey serum in PBS, and then the samples were subjected to probing with the appropriate primary antibodies at 4 °C overnight. The samples were then incubated with Fluorescein (FITC)-conjugated secondary antibodies (Jackson Laboratory, Bar Harbor, ME) for one hour at room temperature. The nuclei were counterstained with DAPI (Sigma) and β-actin with Phalloidin. The fluorescence was visualized under confocal microscopy (Leica).

2.7. Western blot analysis

Cell lysates were extracted with cell lysis buffer (Beyotime, China) and the protein concentration in the lysates was quantified using an Enhanced BCA Protein Assay Kit (Beyotime, China). Protein samples with 30–50 μg were loaded for immunoblotting (IB), using antibodies against p16, pCHK2, pBRCA1, pH2A, CDK6 (Cell Signaling Inc, USA), P53, p21 (Epitomics, China), pRb (Santa Cruz Biotechnology, USA), and Actin (Kangwei, China).

2.8. Immunohistochemistry

Formalin-fixed tissues were paraffin embedded, and 5-μm sections were placed on slides. Before immunostaining, the paraffin sections were deparaffinized, rehydrated, fixed and subjected to antigen retrieval in 0.05% proteinase K. Then the slides were blocked in 10% donkey serum in PBS for 1 h and incubated in appropriate primary antibodies at 4 °C overnight. The following procedures were performed with a Mouse and Rabbit Specific HRP/DAB detection IHC kit (ab64264, abcam) according to the manufacturer's instructions, and hematoxylin was used as a counterstain. All sections were visualized under the microscope (OLYMPUS IX71, Tokyo, Japan).

2.9. Statistical analysis

All data are displayed as mean ± SD (standard deviation) values. Student's *t*-test was applied to study the relationship between the different variables. $P < 0.05$ was considered statistically significant.

3. Results

3.1. Extracellular adenosine suppresses the growth of lung cancer cells in vitro and in vivo

To examine the role of adenosine in the growth of lung cancer cells, we recorded the confluence changes of the cells every two

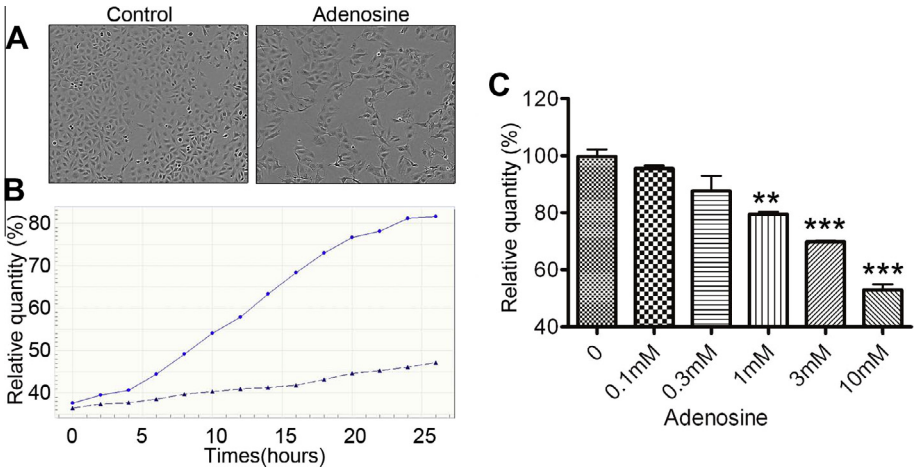

Fig. 1. The growth suppressive effect of adenosine on lung cancer cells *in vitro*. (A and B) Representative growth curves of cells untreated or treated with adenosine at a concentration of 10 mM. Each curve was performed at least four times, and each time point was determined in triplicate. (C) A549 cells were analyzed for cell viability by a MTT assay. The results are displayed as mean ± SD values from four replicate wells of three separate experiments.

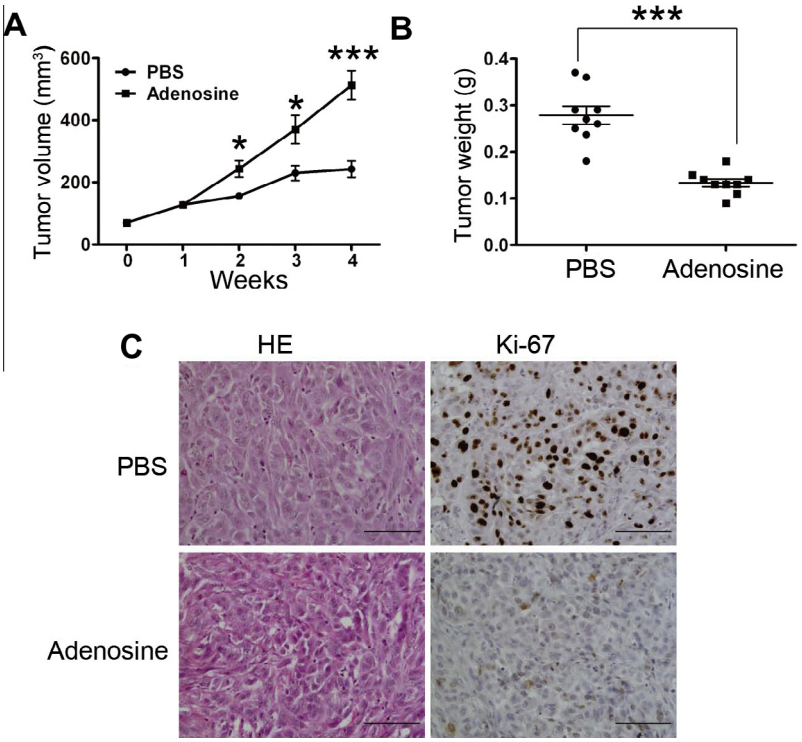

Fig. 2. Adenosine inhibited tumor growth of A549 xenograft *in vivo*. (A) Adenosine inhibited tumor growth of A549 xenograft. Points represent mean values ($n = 10$); bars represents SD. (B) Adenosine reduced tumor weight. At the end of the experiment, tumors from the mice were dissected and weighed, and the average tumor weight was calculated and expressed as mean ± SD ($n = 10$, $^{***}p < 0.001$). (C) Tumor sections were detected by hematoxylin and eosin staining, immunochemical analysis for ki67 (Scale bars: 100 μm).

hours in the wells of culture plates and observed their growth curve by the live-cell imaging system IncuCyte™. We found that after a 24 h treatment with adenosine, the growth of A549 cells was dramatically decreased compared with that of the untreated control group, in which cells grew until confluence (Fig. 1A and B). Also, in the MTT assay, extracellular adenosine reduced A549 cell viability in a concentration (0.1–10 mM) dependent manner, reaching nearly 50% of control levels after 24 h treatment with 10 mM adenosine (Fig. 1C).

We next evaluated the anti-tumor effect of adenosine *in vivo* by using an A549 xenograft mouse model. As shown in Fig. 2A, the tumor growth in the adenosine group was significantly inhibited by 50% compared with that of the PBS control group. The average tumor weight in the adenosine group was also significantly decreased (Fig. 2B). Furthermore, H&E staining revealed elongated cell morphology in the xenografted tumor tissue from mice treated with adenosine. We also did staining of the xenograft tumor tissue with Ki67, a proliferating cell marker, and found that the Ki67 (+) cells were decreased in the tissues treated with adenosine (Fig. 2C). Taken together, these findings demonstrate that adenosine significantly suppresses the growth of lung cancer cells both *in vitro* and *in vivo*.

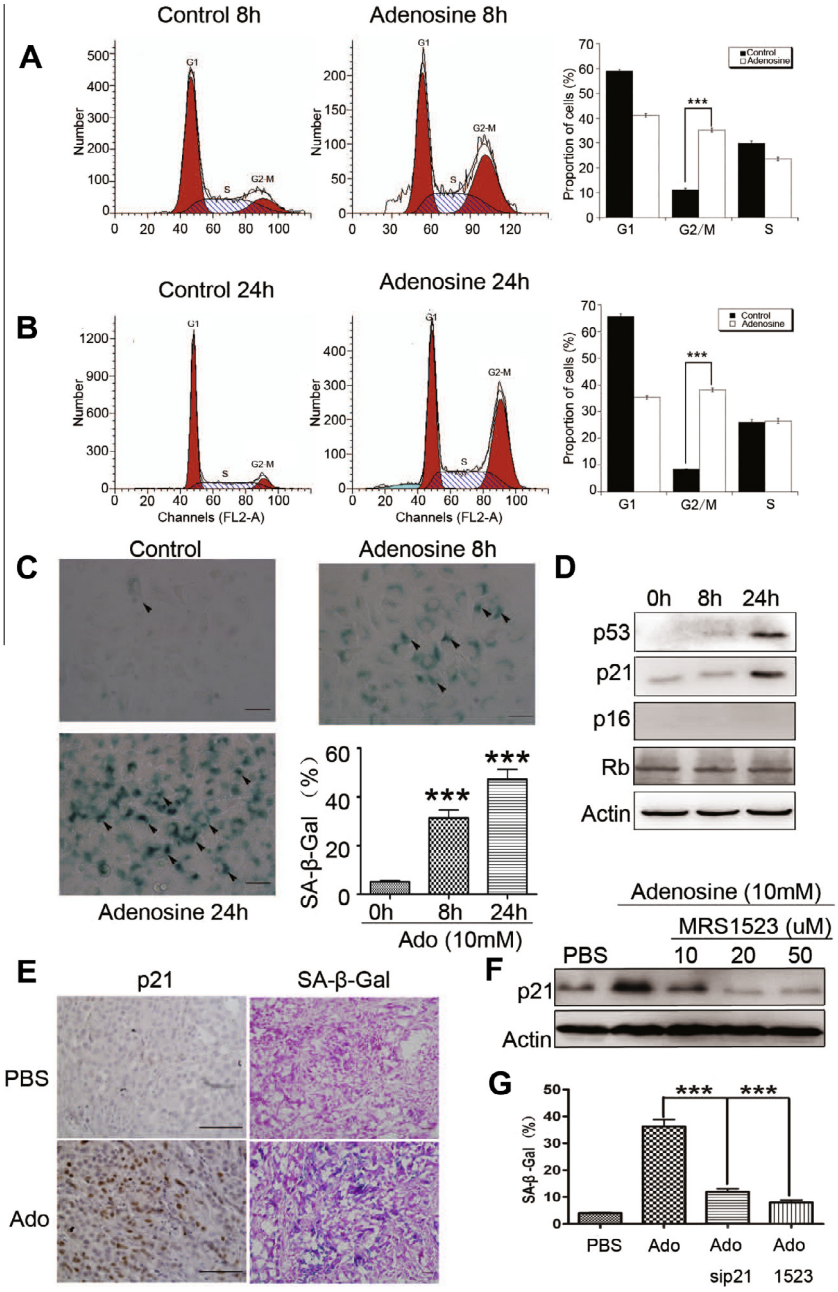

Fig. 3. Adenosine induced G2/M cell cycle arrest and p21-dependent cell senescence. (A and B) Adenosine induced G2/M cell cycle arrest for 8 h (A) and 24 h (B). Cells were treated with 10 mM adenosine for 8 h or 24 h, subjected to PI staining and FACS analysis to determine cell cycle profile. The right graph shows the percentages of cells. Values are means ± SD of three independent experiments (***$p < 0.001$). (C) Adenosine induced cell senescence *in vitro*. Cells were untreated or treated with 10 mM adenosine. Scale bar, 20 μm. The lower right graph shows the percentages of SA-β-Gal positive cells. Values are means ± SD of three independent experiments. (D) Adenosine-induced cell senescence is p53/p21-dependent in A549 cells. The A549 cells were treated with adenosine for 8 h or 24 h and were subjected to IB analysis of expression of proteins indicated with actin as a loading control. (E) Adenosine also induced cell senescence *in vivo*. Tumor sections were detected by SA-β-Gal staining and immunochemical analysis for p21 (Scale bars: the left panels are 100 μm, the right panels are 20 μm). (F) MRS1523 inhibited adenosine-induced p21 accumulation. The cells were treated with adenosine or MRS for 24 h and subjected to IB analysis. (G) Adenosine-induced cell senescence is p21-dependent in A549 cells. The cells were transfected with sip21 or control siRNA for 72 h or treated with 50 μM MRS1523 and 10 mM adenosine for 24 h then subjected to senescence analysis with SA-β-gal staining. The results are presented as mean value ± SE from three independent experiments,***$p < 0.001$.

3.2. Extracellular adenosine induces G2/M cell cycle arrest and p21-dependent cell senescence

To understand the mechanism underlying the adenosine-induced growth suppression in lung cancer cells, we initially explored the cell cycle profile in adenosine-treated A549 cells with PI staining. Adenosine induced G2-M arrest which occurred at 8 h (Fig. 3A), and reached a peak at 24 h (Fig. 3B) in A549 cells. Moreover, we recorded the cell cycle changes every twenty minutes by the live-cell imaging system IncuCyte™ and found that cells division was clearly observed in PBS control group but the cell cycle progress was completely inhibited upon adenosine treatment (data not shown). Morphologically, adenosine-treated cells were much larger in size with flattened shape, a feature of cell senescence, compared with control cells (Fig. 1A). To determine whether adenosine indeed induced senescence, we examined the expression of senescence-associated β-galactosidase (SA-β-gal), a classic biochemical marker for cellular senescence. We found that about

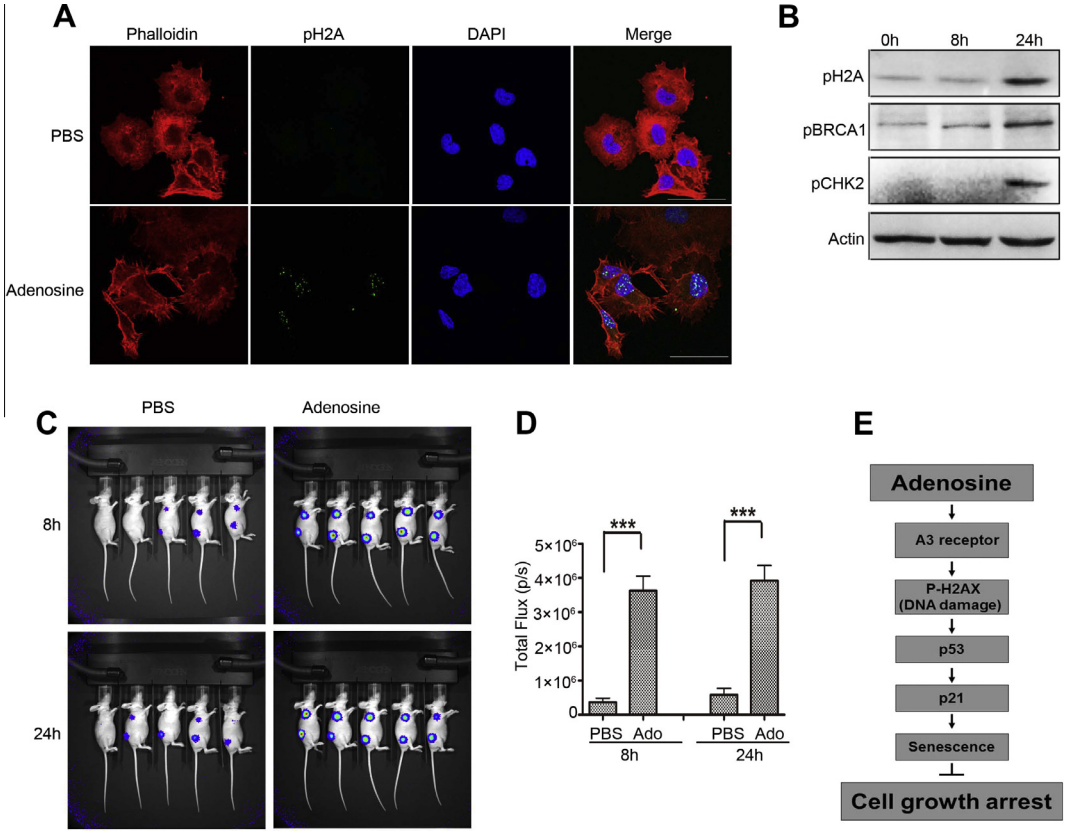

Fig. 4. Adenosine induced p53 activation by triggering cellular DNA damage signal. (A) Immunofluorescence microscopy on A549 cells treated with 10 mM adenosine for 24 h. DDR activation is indicated by phosphorylation of H2AX (green). The nucleus was stained with DAPI (blue) and β-actin was stained with Phalloidin (red). Scale bar, 50 μm. (B) Adenosine induced activation of DNA damage signal. Cells were treated with 10 mM adenosine for 8 h or 24 h and subjected to IB analysis for expression of proteins indicated. (C) Molecular imaging of the p53 activity after adenosine treatment *in vivo*. A549 cells containing the p53-RE-luc construct were implanted subcutaneously in nude mice. The mice were injected with adenosine (i.p. 50 mg/kg) and then imaged at 8 h and 24 h. (D) The strongest activated bioluminescent signal was found at 8 h or 24 h in the adenosine treated group compared with the PBS group (***$p < 0.001$). (E) Working model. Adenosine induces p21-dependent senescence to suppress the growth of lung cancer cells through the adenosine A3 receptor, activating DNA damage response signaling. (For interpretation of the references to colour in this figure legend, the reader is referred to the web version of this article.)

48% of adenosine-treated cells, but less than 5% of control cells, were positively stained (Fig. 3C). These findings indicate that cells arrested at the G2/M upon adenosine treatment eventually undergo senescence.

To address how adenosine induces senescence in the cells, we determined the activation status of the p16/pRB and p53/p21 axes and found that adenosine induces the accumulation of p53 and p21, but not pRB and p16, in A549 lung cancer cells (Fig. 3D). We also examined the expression of p21 and β-galactosidase (SA-β-gal) in xenografted tumor tissues and found their expression was dramatically increased in the adenosine treatment group compared with the control group (Fig. 3E). We found that adenosine-induced increase of p21 expression could be blocked by treatment with A3 receptor antagonist, MRS1523 (Fig. 3F). Moreover, knockdown of p21 and MRS1523 treatment significantly blocks the adenosine-induced increase of SA-β-gal (+) cells (Fig. 3G). Also, p21 knockdown significantly blocks adenosine induced G2-M cell cycle arrest in the cells (Supplementary fig. 1). These results indicate that adenosine induces cellular senescence in a p53/p21-dependent manner and through activation of the adenosine A3 receptor.

3.3. Extracellular adenosine increases phosphor-γH2AX, pCHK2 and pBRCA1

To further understand how adenosine induces the p53/p21 activation, we did immunofluorescence staining of phosphor-γH2AX, and found that the positive phosphor-γH2AX staining was observed in adenosine-treated cells (Fig. 4A). We further performed a time course study on adenosine-induced change of phosphor- γH2AX and found that the levels of phosphor-γH2AX reach a peak at 24 h post-treatment with adenosine, which is consistent with the senescence in cells. We also determined the level of pCHK2 and pBRCA1 upon adenosine treatment of the cells and found that they were significantly increased and reached a peak 24 h after adenosine treatment (Fig. 4B).

We then observed the adenosine-induced changes of p53 activity with a p53-RE-Fluc/A549 reporter cell line and found that the fluc activity of p53-RE-Fluc/A549 cells was significantly increased after 10 mM adenosine treatment for 8 h or 24 h (Supplementary fig. 2). We further observed the adenosine-induced dynamic changes of p53 activity *in vivo* using living imaging in a mouse model with xenografted p53-RE-Fluc/A549 reporter cells and found that a much stronger bioluminescent signal was detected at 8 h and reached a peak at 24 h in the adenosine-treated group compared with that of PBS control groups (Fig. 4C and D, $n = 10$). These data suggest that adenosine-induced p53 activation may result from increase of phosphor-γH2AX, pCHK2 and pBRCA1, the index of DNA damage response.

4. Discussion

The results of the present study demonstrate that extracellular adenosine suppresses A549 lung cancer cell growth via induction of senescence in a p53/21 dependent manner and which may be

initiated by the increase of phosphor-γH2AX, pCHK2 and pBRCA1, the markers for DNA damage response.

Cellular senescence is a mechanism to restrain proliferation of potentially tumorigenic cells, and induction of senescence in cancer cells has become a promising approach for cancer therapy [13,14]. We reported that the ROC1 knockdown-induced senescence in liver cancer cells is largely dependent on p21, since p21 is significantly induced in response to ROC1 knockdown, and simultaneous knockdown of p21 remarkably abrogated this senescence [15]. In this study, we found that cell senescence induced by adenosine contributes to the growth suppression of lung cancer cells. Adenosine activates p53/p21 and knockdown of p21 blocks adenosine-induced senescence and cell cycle arrest. This indicates that adenosine induces senescence in a p53/p21 dependent manner. We also found that adenosine increases phosphor-γH2AX, pCHK2, and pBRCA1. These findings suggest a new model that extracellular adenosine induces cellular senescence in a p53/p21 dependent manner and may be triggered by a similar signaling pathway as DNA damage response (Fig. 4E).

The most commonly described signaling pathway for drug induced cell growth arrest is initiated by DNA damage [11]. Major cancer drugs such as the topoisomerase inhibitors, doxorubicin, etoposide, campthothecin, and alkylating agents such as cisplatin and BCNU have been reported to induce DNA damage, particularly DNA double-strand breaks (DSBs) [16–18]. DNA damage results in the activation of ATM and ATR, members of the phosphatidylinositol 3-kinase-related kinases (PIKK), and propagation of the signal through phosphorylation and activation of downstream intermediates including H2AX, NBS1 and BRCA1, which in turn lead to activation of Chk1 and Chk2 and cell cycle arrest. Cell cycle arrest in response to DNA damage allows for repair before cell cycle progression is resumed, or, if the damage is too extensive, senescence or even apoptosis may be triggered. The most fundamental event of the drug-induced G1-S checkpoint is the stabilization of p53, leading to enhanced transcription of p21/WAF1 and growth arrest. We found that adenosine increases phosphor-γH2AX, pCHK2, pBRCA1, along with an increase of p53 activity and p21 expression, indicating they are responsible for initiation of adenosine-induced cell cycle arrest and senescence in cells.

Senescence induction is coupled with DNA damage in a p53/p21-dependent manner in human cancer cells. Extracellular adenosine induces cellular senescence through p53/p21 activation and that the adenosine-induced increase of phosphor-γH2AX pCHK2 and pBRCA1 may initiate the process. However, how adenosine causes the increase of phosphor-γH2AX needs to be further clarified. The adenosine A3 receptor antagonist, MRS1523 could rescue blocks adenosine-induced senescence. These results may suggest that activation of adenosine via the A3 receptor results in the phosphorylation of γH2AX via activation of unknown protein kinase(s).

In summary, adenosine induces senescence of human lung cancer cells in a p53/p21-dependent manner. This study reveals a novel mechanism for extracellular adenosine induced cell growth arrest and provides further experimental evidence of adenosine acting as an effective anticancer agent.

Acknowledgments

This work is supported by the Shanghai Committee of Science and Technology of China to Jie Liu (Grant No.12JC1402000 and 12410705300); also supported partially by Four diamond foundation of Pennsylvania State University, USA, to Chunhua Song and Sinisa Dovat. We thank Sadie Hogan and Marie S. Bulathsinghala for their proof reading for English grammar.

Appendix A. Supplementary data

Supplementary data associated with this article can be found, in the online version, at http://dx.doi.org/10.1016/j.bbrc.2013.09.030.

References

[1] D. Yang, T. Yaguchi, H. Yamamoto, T. Nishizaki, Intracellularly transported adenosine induces apoptosis in HuH-7 human hepatoma cells by downregulating c-FLIP expression causing caspase-3/-8 activation, Biochem. Pharmacol. 73 (2007) 1665–1675.
[2] M. Saitoh, K. Nagai, K. Nakagawa, T. Yamamura, S. Yamamoto, T. Nishizaki, Adenosine induces apoptosis in the human gastric cancer cells via an intrinsic pathway relevant to activation of AMP-activated protein kinase, Biochem. Pharmacol. 67 (2004) 2005–2011.
[3] D. Yang, T. Yaguchi, C.-R. Lim, Y. Ishizawa, T. Nakano, T. Nishizaki, Tuning of apoptosis-mediator gene transcription in HepG2 human hepatoma cells through an adenosine signal, Cancer Lett. 291 (2010) 225–229.
[4] M.H. Linskens, J. Feng, W.H. Andrews, B.E. Enlow, S.M. Saati, L.A. Tonkin, W.D. Funk, B. Villeponteau, Cataloging altered gene expression in young and senescent cells using enhanced differential display, Nucleic Acids Res. 23 (1995) 3244–3251.
[5] D.N. Shelton, E. Chang, P.S. Whittier, D. Choi, W.D. Funk, Microarray analysis of replicative senescence, Curr. Biol. 9 (1999) 939–945.
[6] C.B. Harley, A.B. Futcher, C.W. Greider, Telomeres shorten during ageing of human fibroblasts, Nature 345 (1990) 458–460.
[7] M. Serrano, A.W. Lin, M.E. McCurrach, D. Beach, S.W. Lowe, Oncogenic ras provokes premature cell senescence associated with accumulation of p53 and p16INK4a, Cell 88 (1997) 593–602.
[8] R.H. te Poele, A.L. Okorokov, L. Jardine, J. Cummings, S.P. Joel, DNA damage is able to induce senescence in tumor cells *in vitro* and *in vivo*, Cancer Res. 62 (2002) 1876–1883.
[9] J.W. Shay, I.B. Roninson, Hallmarks of senescence in carcinogenesis and cancer therapy, Oncogene 23 (2004) 2919–2933.
[10] J.R. Smith, O.M. Pereira-Smith, Replicative senescence: implications for *in vivo* aging and tumor suppression, Science 273 (1996) 63–67.
[11] A. Rebbaa, Targeting senescence pathways to reverse drug resistance in cancer, Cancer Lett. 219 (2005) 1–13.
[12] A. Hirao, DNA damage-induced activation of p53 by the checkpoint kinase Chk2, Science 287 (2000) 1824–1827.
[13] C.A. Schmitt, J.S. Fridman, M. Yang, S. Lee, E. Baranov, R.M. Hoffman, S.W. Lowe, A senescence program controlled by p53 and p16INK4a contributes to the outcome of cancer therapy, Cell 109 (2002) 335–346.
[14] J. Campisi, F. d'Adda di Fagagna, Cellular senescence: when bad things happen to good cells, Nat. Rev. Mol. Cell Biol. 8 (2007) 729–740.
[15] D. Yang, L. Li, H. Liu, L. Wu, Z. Luo, H. Li, S. Zheng, H. Gao, Y. Chu, Y. Sun, J. Liu, L. Jia, Induction of autophagy and senescence by knockdown of ROC1 E3 ubiquitin ligase to suppress the growth of liver cancer cells, Cell Death Differ. 20 (2013) 235–247.
[16] W.E. Ross, M.O. Bradley, DNA double-stranded breaks in mammalian cells after exposure to intercalating agents, Biochim. Biophys. Acta 654 (1981) 129–134.
[17] D.H. Lau, A.D. Lewis, M.N. Ehsan, B.I. Sikic, Multifactorial mechanisms associated with broad cross-resistance of ovarian carcinoma cells selected by cyanomorpholino doxorubicin, Cancer Res. 51 (1991) 5181–5187.
[18] J.P. Banath, P.L. Olive, Expression of phosphorylated histone H2AX as a surrogate of cell killing by drugs that create DNA double-strand breaks, Cancer Res. 63 (2003) 4347–4350.